







Symbiont Genomic Features and Localization in the Bean Beetle *Callosobruchus maculatus*

 Aileen Berasategui,^a  Abraham G. Moller,^b Benjamin Weiss,^c Christopher W. Beck,^a Caroline Bauchiero,^a  Timothy D. Read,^{a,b} Nicole M. Gerardo,^a  Hassan Salem^{a,d}

^aDepartment of Biology, Emory University, Atlanta, Georgia, USA

^bDivision of Infectious Diseases, Emory University School of Medicine, Atlanta, Georgia, USA

^cDepartment of Evolutionary Ecology, Johannes Gutenberg University, Mainz, Germany

^dMutualisms Research Group, Max Planck Institute for Developmental Biology, Tübingen, Germany

ABSTRACT A pervasive pest of stored leguminous products, the bean beetle *Callosobruchus maculatus* (Coleoptera: Chrysomelidae) associates with a simple bacterial community during adulthood. Despite its economic importance, little is known about the compositional stability, heritability, localization, and metabolic potential of the bacterial symbionts of *C. maculatus*. In this study, we applied community profiling using 16S rRNA gene sequencing to reveal a highly conserved bacterial assembly shared between larvae and adults. Dominated by *Firmicutes* and *Proteobacteria*, this community is localized extracellularly along the epithelial lining of the bean beetle's digestive tract. Our analysis revealed that only one species, *Staphylococcus gallinarum* (phylum *Firmicutes*), is shared across all developmental stages. Isolation and whole-genome sequencing of *S. gallinarum* from the beetle gut yielded a circular chromosome (2.8 Mb) and one plasmid (45 kb). The strain encodes complete biosynthetic pathways for the production of B vitamins and amino acids, including tyrosine, which is increasingly recognized as an important symbiont-supplemented precursor for cuticle biosynthesis in beetles. A carbohydrate-active enzyme search revealed that the genome codes for a number of digestive enzymes, reflecting the nutritional ecology of *C. maculatus*. The ontogenic conservation of the gut microbiota in the bean beetle, featuring a "core" community composed of *S. gallinarum*, may be indicative of an adaptive role for the host. In clarifying symbiont localization and metabolic potential, we further our understanding and study of a costly pest of stored products.

IMPORTANCE From supplementing essential nutrients to detoxifying plant secondary metabolites and insecticides, bacterial symbionts are a key source of adaptations for herbivorous insect pests. Despite the pervasiveness and geographical range of the bean beetle *Callosobruchus maculatus*, the role of microbial symbioses in its natural history remains understudied. Here, we demonstrate that the bean beetle harbors a simple gut bacterial community that is stable throughout development. This community localizes along the insect's digestive tract and is largely dominated by *Staphylococcus gallinarum*. In elucidating symbiont metabolic potential, we highlight its possible adaptive significance for a widespread agricultural pest.

KEYWORDS host-microbe, symbiosis, bean beetle, insect, herbivory

The bean beetle *Callosobruchus maculatus* (Coleoptera: Chrysomelidae: Bruchidae) is a prolific pest of stored leguminous grains (1). Originating in the Old World, members of the *Callosobruchus* genus presently inhabit every continent owing to a global dispersal network that is largely facilitated by agricultural commerce (2).

Citation Berasategui A, Moller AG, Weiss B, Beck CW, Bauchiero C, Read TD, Gerardo NM, Salem H. 2021. Symbiont genomic features and localization in the bean beetle *Callosobruchus maculatus*. *Appl Environ Microbiol* 87:e00212-21. <https://doi.org/10.1128/AEM.00212-21>.

Editor Karyn N. Johnson, University of Queensland

Copyright © 2021 American Society for Microbiology. All Rights Reserved.

Address correspondence to Aileen Berasategui, aberas2@emory.edu, or Hassan Salem, hassan.saleem@tuebingen.mpg.de.

Received 28 January 2021

Accepted 1 April 2021

Accepted manuscript posted online

16 April 2021

Published 26 May 2021

Exploiting leguminous seeds throughout cultivation, storage, and transport, *C. maculatus* drastically limits grain yields in both industrial and backyard cropping systems (3). Numerous grain varieties belonging to the Fabaceae are susceptible to infestations by *C. maculatus* (4), including mung (*Vigna radiata*), adzuki (*Vigna angularis*), cowpea (*Vigna unguiculata*), pigeon pea (*Cajanus cajan*), and hyacinth beans (*Lablab purpureus*). Similar to other bruchid species, *C. maculatus* females oviposit on grains by exuding a protective secretion to fixate and attach the egg onto the seed coat (5). Upon hatching, emerging larvae burrow into the seed and complete their development entirely within the grain, consuming ~11% of its overall mass (6). With a life cycle spanning 4 weeks, breakouts of *C. maculatus* in granaries can halve the overall weight of stored products within 3 to 5 months (7). Beyond compromising the commercial value of pulses, the preference of *Callosobruchus* larvae for seeds' cotyledons drastically arrests germination (8), contributing to thousands of tons of spoiled produce annually (4).

Reflecting the pervasiveness of *C. maculatus* and the experimental tractability afforded from short generation times under laboratory settings (9), numerous aspects of the beetle's reproductive cycle, developmental biology, and behavioral ecology have been elucidated (10–13). The resident microbiome of *C. maculatus*, in contrast, remains understudied.

Bacterial symbionts allow many insect lineages to thrive on important crops, with contributions that range from insecticide resistance to the detoxification of noxious plant secondary compounds or the supplementation of limiting nutrients (14–16, 78). For example, the coffee berry borer (*Hypothenemus hampei*) harbors a conserved gut microbiome that helps the beetle overcome the antiherbivory effects of caffeine by detoxifying the alkaloid (17). Similarly, the bean bug *Riptortus pedestris* is able to withstand exposure to fenitrothion, an insecticide, through the degradative capacity of its environmentally acquired *Burkholderia* symbionts (14). Among grain feeders, the beetles *Sitophilus oryzae* and *Oryzaephilus surinamensis* subsist entirely on cereals deficient in amino acids by partnering with bacteriome-localized endosymbionts. Symbiont supplementation of aromatic amino acids (e.g., phenylalanine and tyrosine) is critical for cuticle biosynthesis in both of these hosts, evidenced by aposymbiotic beetles exhibiting paler coloration, thinner cuticles, and lower body mass (18–20). Notably, aposymbiotic *O. surinamensis* beetles suffer low survivorship but only under dry conditions (20). As low ambient humidity characterizes most granaries, symbiont contributions may secondarily underlie the ability of some stored product pests to contend with anthropogenic pressures and thrive in dry storage facilities designed to prevent the growth of mold fungi (20).

Previous studies characterizing the bacterial community associated with *C. maculatus* focused exclusively on the adult stage. Through culture-dependent (21) and -independent (22) approaches, these efforts point to adult beetles consistently partnering with bacterial symbionts belonging to the genera *Staphylococcus*, *Enterococcus*, *Pseudomonas*, and *Enterobacter*. However, how conserved is this community throughout the developmental cycle of *C. maculatus*? Where do these symbionts localize within the host? And which metabolic features do they encode? In this study, we combine 16S rRNA gene profiling, microscopy, and whole-genome sequencing to determine the conservation, localization, heritability, and metabolic potential of the core bacterial community associated with *C. maculatus*.

RESULTS AND DISCUSSION

***Callosobruchus maculatus* harbors a simple, heritable bacterial community throughout development.** The bacterial community of the bean beetle *C. maculatus* was characterized throughout development using Illumina amplicon sequencing of the bacterial 16S rRNA gene. A total of 480,536 high-quality sequences were generated across 20 samples representing eggs, larvae, and adults. These sequences were subsequently binned to 425 amplicon sequence variants (ASVs) (100% sequence similarity). After taxonomic assignment, 42 ASVs were removed because they were classified as chloroplasts (23) or *Archaea* (5). The 5 ASVs assigned to *Archaea* belonged to the

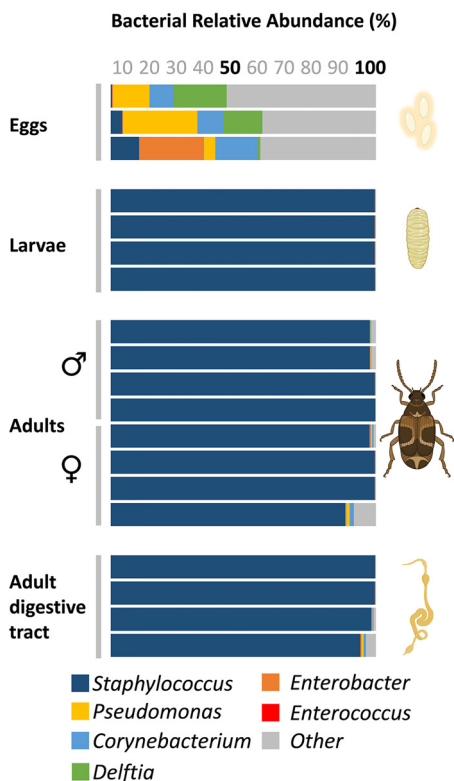


FIG 1 *C. maculatus* harbors a simple gut microbial assembly that is representative of the beetle’s overall bacterial community and is largely stable throughout development. (A) Genus-level gut bacterial community composition of *C. maculatus* across different developmental stages, sexes, and body sites. Each bar corresponds to one sample with pooled individuals. “Adult” refers to whole adults, including the digestive tract.

YLA114 phylum and were detected in just one egg sample, comprising 5% of all reads within the sample. The rarity of these microbes within bean beetles, in addition to their presence in nonscarabaeoid beetles being unusual, suggests that *Archaea* may be a contaminant in this sample.

The remaining 383 ASVs contained an average of 24,129 reads per sample, representing 95.4% of the original sequences (see Table S1 in the supplemental material). These ASVs were assigned to 91 bacterial species spanning 81 genera (97% and 95% ASV similarities, respectively). Eggs more commonly associate with *Proteobacteria*, followed by *Actinobacteria*, *Firmicutes*, and *Bacteroidetes*, whereas larvae and adults largely harbor *Firmicutes* and, to a lesser extent, *Proteobacteria* (Table S2). The bacterial communities of larvae and adults, compositionally simple, are predominantly represented by *Staphylococcus*, *Enterococcus*, and *Enterobacter* (Fig. 1). The high relative abundance of *Staphylococcus* in larvae and adults is especially notable, ranging between 99.5% and 97.6% of the total sequences per sample, respectively (Fig. 1). This is consistent with culture-dependent approaches pointing to *Staphylococcus* as the most common bacterial genus consistently isolated from *C. maculatus* (21, 24).

Several distance metrics were calculated to assess the variation in bacterial community structure between sexes, body sites (whole body versus digestive tract), and developmental stages. Beta diversity analyses based on weighted UniFrac distance matrices (Table S3) revealed that the microbiota composition of the beetle host does not differ between sexes (pseudo-*F* = 1.01 and *P* = 0.44 by permutational multivariate analysis of variance [PERMANOVA]). Likewise, no variation in community composition was observed between body sites (pseudo-*F* = 0.21 and *P* = 0.45 by PERMANOVA), confirming that the gut bacterial community is indeed representative of the adult beetle as a whole, as has been described for other insect groups (25). However, there is significant

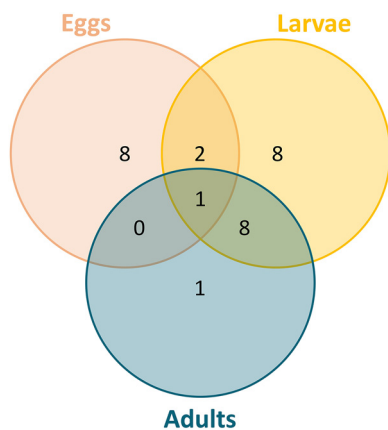


FIG 2 Only one species (i.e., a single 16S ASV), *Staphylococcus gallinarum*, constitutes the core microbiome, being shared across all samples spanning all developmental stages. A Venn diagram representing the number of shared and exclusive bacterial amplicon sequence variants (100% similarity) in *C. maculatus* samples across development is shown. Only strains present in 100% of the samples of each type are depicted.

variation between developmental stages. The most significant variation that we observe compositionally is that for eggs relative to larvae and adults (pseudo- $F = 13.72$ and $q = 0.03$, and pseudo- $F = 45.86$ and $q = 0.006$, respectively, by pairwise PERMANOVA). The latter two do not differ from each other (pseudo- $F = 1.35$ and $q = 0.29$ by pairwise PERMANOVA). Overall, these results are consistent with those obtained from the other distance matrices tested, Bray-Curtis and Jaccard (Table S3).

An analysis of the “core microbiome” (i.e., those ASVs shared by 100% of all samples) revealed that just one ASV is maintained throughout the developmental cycle of *C. maculatus* (Fig. 2). Phylogenetic placement (see below) classified this ASV as *Staphylococcus gallinarum*. While the transmission route was not directly elucidated, the presence of this ASV in every sample across all developmental stages suggests that *S. gallinarum* is vertically transmitted from mother to offspring in the bean beetle.

The differences in bacterial diversity observed throughout development are most severe between the egg and larval stages of *C. maculatus*. While this may stem from uneven sampling depth, it could also reflect the development of the gut as a habitat to house a specialized community adapted to the unique physicochemical conditions forming along the digestive tract (26). These conditions can vary substantially in both pH and oxygen availability (25, 27), potentially sieving environmental microbes conditioned to the aerobic surfaces on the egg. The compositional stability observed post-closure in *C. maculatus* may also reflect a specific and consistent immune profile in both larvae and adults (26), which can confer tolerance to commensal or beneficial members (28, 29) while eliminating environmental or pathogenic strains (30).

***S. gallinarum* lines the foregut digestive tract of *C. maculatus*.** As 16S rRNA gene profiling revealed that the bacterial community inhabiting the digestive tract of *C. maculatus* is representative of the beetle as a whole, we aimed to localize the symbiont along the insect’s gut using fluorescence *in situ* hybridization (FISH). Performed on representative semi-thin sections of the digestive system, FISH revealed that bacterial colonization in the gut is largely restricted to the foregut, evidenced by the clear, dual fluorescence of eubacterial and *S. gallinarum*-specific probes in this region but not in the midgut or hindgut (Fig. 3). Within the foregut, symbiont localization is exclusively extracellular along the epithelial lining, with limited bacterial presence in the lumen. The overlapping fluorescence of the *S. gallinarum*-specific probe (Cy5) and the general eubacterial probe (Cy3) is consistent with 16S rRNA gene profiling of the digestive tract revealing that the gut bacterial community is largely dominated by the firmicute.

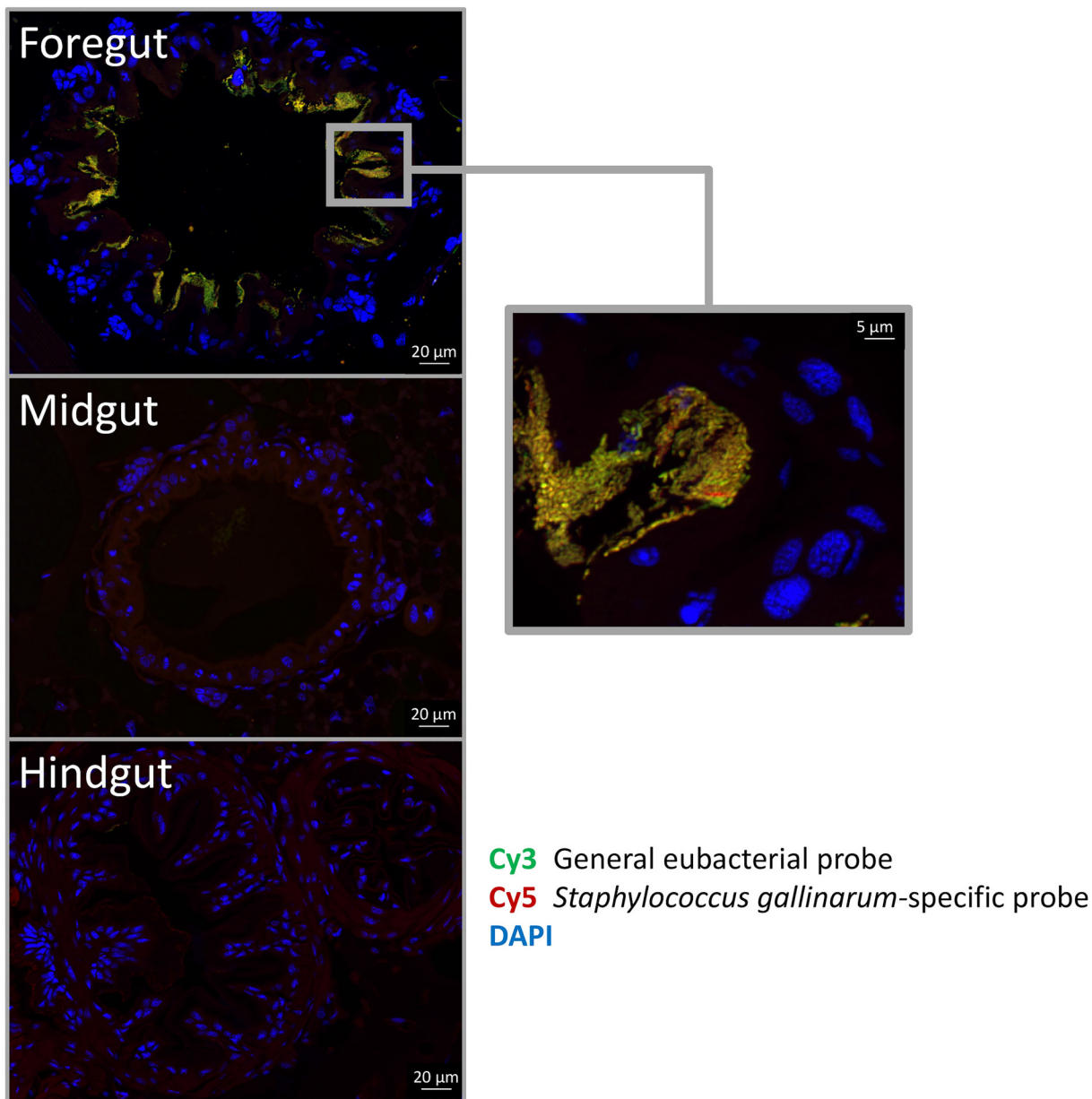


FIG 3 *S. gallinarum* locates extracellularly and lines the foregut epithelium in *C. maculatus*. Transversal cross-section fluorescence *in situ* hybridization of *C. maculatus*' foregut, midgut, and hindgut targeting the 16S rRNA gene of *Staphylococcus gallinarum* (red) and general eubacteria (green). DAPI (blue) was used for counterstaining. Scale bars are included for reference.

Genomic features and phylogenetic placement of *C. maculatus*-associated *S. gallinarum*. Whole-genome sequencing of *S. gallinarum* isolated from the beetles' digestive tract was carried out to understand the biological role of the symbiont within *C. maculatus*' gut. A hybrid assembly of long MinION and short Illumina reads yielded a contiguous and circularized genome with general features that are consistent with those of other members of the *Staphylococcus* genus (31). The bacterial symbiont harbors one chromosome (2.89 Mb; 33% GC content) (Fig. 4A and B) and one plasmid (46 kb; 28% GC content). The direction of gene transcription is asymmetrical with respect to the vertical axis of the genome map (Fig. 4A). The change in direction is observed around half past 6, which is supported by GC skew values. This observation suggests that the replication termination site of *C. maculatus*-associated *S. gallinarum* is located around the 195° position on the genome map and not directly opposite the replication

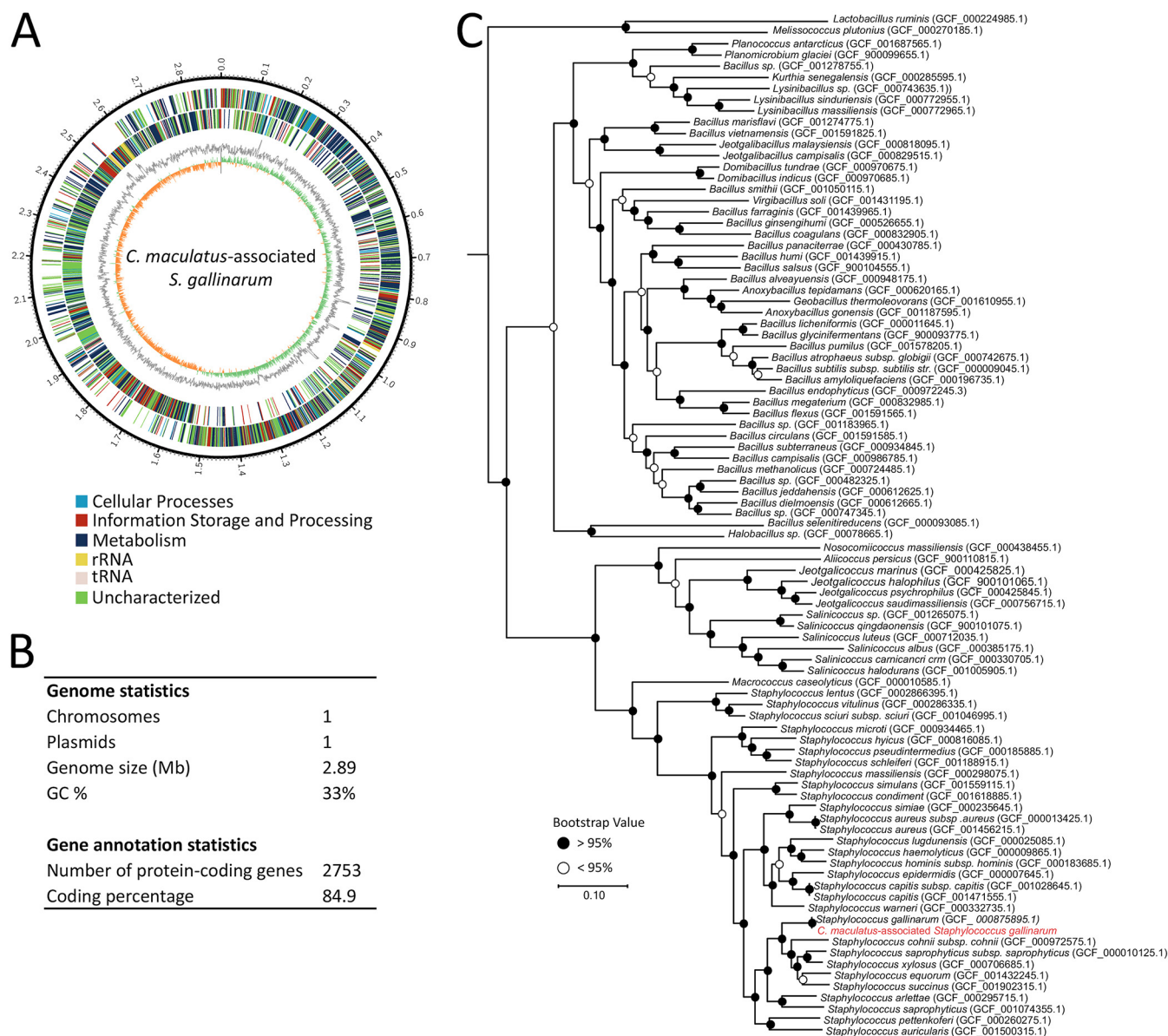


FIG 4 Genomic features and phylogenetic placement of *C. maculatus*-associated *S. gallinarum*. (A) Circular view of the *C. maculatus*-associated *S. gallinarum* genome. Internal coding sequence (CDS) circles indicate annotated functional COG categories differentiated by coloration and found in the positive (outer circle) or negative (inner circle) strand. The gray ring denotes the relative GC content. The innermost ring represents GC skew values. (B) Genome structure and annotation statistics. (C) Phylogenetic placement of *C. maculatus*-associated *Staphylococcus gallinarum* within the Firmicutes phylogeny. RefSeq accession numbers are in parentheses.

origin, resulting in two replichores of different lengths. This lack of symmetry is common in bacteria and often correlates with the enrichment of the leading replicating strand in essential genes, which are also more conserved than genes in the lagging strand (32). In *Staphylococcus* sp., the leading strand can additionally contain horizontally acquired genes coding for traits specific to each strain within a species (33).

Staphylococcus strains, historically characterized as human pathogens, are classified by their ability to coagulate blood into coagulase-positive and -negative strains. Whereas *Staphylococcus aureus* normally presents a symmetrical GC skew across the vertical axis of the genome map, other strains within the genus, such as *S. saprophyticus*, *S. lugdunensis*, and other coagulase-negative strains, do not (34). *S. gallinarum* is known to be a coagulase-negative species (35), and while a coagulase test was not performed on *C. maculatus*-associated *S. gallinarum*, this bacterium presents the expected GC skew of a coagulase-negative strain. Unlike their coagulase-positive counterparts,

negative strains usually lack aggressive virulence properties and maintain symbiotic interactions with their hosts, colonizing surfaces and mucous membranes of animals (36).

To resolve the phylogenetic placement of *C. maculatus*-associated *S. gallinarum* relative to representative *Firmicutes*, a phylogenomic tree was constructed on the basis of 49 marker genes (Table S4). This confirmed the placement of the beetle's symbiont within the *Staphylococcus* genus and demonstrated that it is most closely related to *Staphylococcus gallinarum*, forming a well-supported monophyletic clade (Fig. 4C). *Staphylococcus gallinarum* was initially isolated and described from a poultry sample (35) and has since been isolated from the skin and respiratory tracts of a number of mammal (37) and insect (23, 38, 39) herbivores. Interestingly, it is yet to be described in the absence of a host.

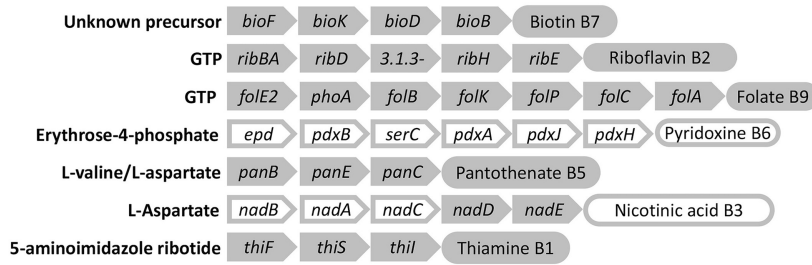
The genome of *C. maculatus*-associated *S. gallinarum* harbors 2,753 putative protein-coding genes, with an average gene size of 892 bp, resulting in a coding percentage of 84.9%. Functional annotation assigned specific functions to 70% of the genes according to the Clusters of Orthologous Groups (COG) database, whereas the rest were assigned to hypothetical proteins or lacked a known function. The genome is equipped with 7 copies of the ribosomal operon containing the 3 structural rRNA genes (5S, 16S, and 23S) and 60 tRNA genes assigning all 20 amino acids. Most genes in the chromosome are involved in metabolic functions (38%), followed by genes involved in information storage and processing (18%) and cellular processes and signaling (11%). Within the metabolic functions, "carbohydrate transport and metabolism" is the most abundant gene category.

Alongside other leaf beetles (Chrysomelidae), *C. maculatus* is a member of the speciose Phytophaga clade of herbivorous beetles. Recent genomic insights into beetle adaptation and diversification revealed that the evolution of specialized herbivory across the coleopteran order, and the origin of the Phytophaga, coincided with the genomic integration of microbial genes encoding plant cell wall-degrading enzymes (PCWDEs) (40, 41). These enzymes, typically glucoside hydrolases (GHs), upgrade the digestive physiology of herbivorous beetles to process a diet rich in recalcitrant polymers such as cellulose, hemicellulose, and pectin (40, 41).

In encoding a subset of pectinases (GH 28) and mannanases (GH 5_10) endogenously, *C. maculatus* is unique, relative to other members of the Phytophaga, in lacking all of the horizontally acquired cellulases belonging to the GH families 9, 45, and 48 (40–42). While *C. maculatus*-encoded mannanases can partially degrade cellulose alongside galactomannan (glucose is an isomer of mannose) (43), most herbivorous beetles deploy multiple cellulolytic enzymes to synergistically monomerize the polysaccharide. As symbiont acquisition can offset the loss of endogenous PCWDEs (44–46), we explored whether *S. gallinarum* might play a similar role for the bean beetle by encoding cellulases to complement the insect's repertoire of endogenous enzymes. In cataloging symbiont-encoded PCWDEs, our annotation revealed 35 enzymatic families (Table S5) putatively involved in the breakdown of plant cell wall polymers. Notably, this included a pair of endoglucanases (GH 6) predicted to internally cleave the β -1,4-glycosidic bonds in cellulose.

Genome annotation revealed the presence of metabolic pathways for the biosynthesis of five B vitamins (Fig. 5A): thiamine (B₁), riboflavin (B₂), pantothenic acid (B₅), biotin (B₇), and folic acid (B₉). The pathway leading to the biosynthesis of nicotinic acid (B₃) from aspartate as a precursor was incomplete, lacking the first three enzymes. Finally, the biosynthetic pathway leading to pyridoxine (B₆) was completely absent. Many seed-based diets are deficient in B vitamin content, necessitating supplementation from specialized endosymbionts (47) or gut bacteria (16). Symbiont-mediated B vitamin supplementation has been demonstrated in grain-feeding beetles, including *Lasioderma serricorne*, *Stegobium paniceum* (48), and *S. oryzae* (49). Similarly, firebugs rely on dietary supplements from their gut-associated *Coriobacteriaceae* symbionts to offset nutritional limitations arising from specializing on cottonseeds deficient in thiamine, riboflavin, pantothenic acid, and pyridoxine (16).

A. B vitamins



B. Essential amino acids

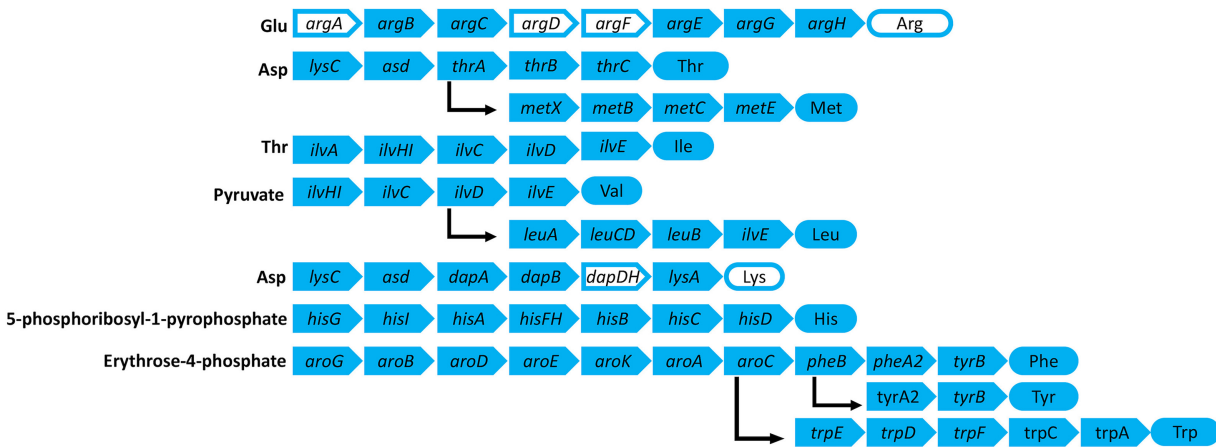


FIG 5 Metabolic pathways for B vitamin biosynthesis (A) and essential amino acids (B) in the genome of *Callosobruchus maculatus*-associated *Staphylococcus gallinarum*. Each arrow represents one step in the biosynthetic pathway. Colored arrows represent a candidate gene for this step that was detected in the annotated genome, whereas white arrows represent candidate genes that were not detected. Rounded boxes represent final products.

Likewise, metabolic pathways involved in the production of essential and aromatic amino acids are present in the genome of *C. maculatus*-associated *S. gallinarum*. In addition to complete pathways for all essential amino acids (except arginine and lysine), *S. gallinarum* encodes a complete shikimate pathway for the biosynthesis of chorismate and prephenate, both precursors of tyrosine (Fig. 5B). Tyrosine is required for the biosynthesis of melanin and catecholamines, which are essential in the tanning and sclerotization of the insect cuticle (50). Given that the shikimate pathway is frequently absent in animals, beetles feeding on deficient diets often rely on bacteria providing tyrosine precursors to build the hardened elytra that are characteristic of these insects (18, 51, 52). Preventing desiccation in dry environments through a strongly sclerotized cuticle, these types of associations may be particularly critical for grain beetles such as *S. oryzae*, *O. surinamensis* (19, 20), and, potentially, *C. maculatus*.

Conclusion. In summary, we show that the simple bacterial community previously described for *C. maculatus* is stable across development and that the microbial assembly along the insect’s digestive tract is representative of the insect’s microbiome as a whole. In characterizing the metabolic features of its sole core member, *S. gallinarum*, we highlight several putatively symbiotic functions toward upgrading the physiology and nutritional ecology of its herbivorous host. Granivorous insects rely on a multitude of metabolic functions from their obligate symbionts, ranging from nutritional supplementation (16, 18–20) to the degradation of recalcitrant or toxic plant compounds (17). The annotation of a complete biosynthetic pathway for the production of tyrosine by *S. gallinarum* is notable given recent findings implicating the symbiont-produced amino acid as an important feature defining numerous beetle-bacterial symbioses, including grain-feeding species belonging to the Silvanidae and Curculionidae

families (18, 20, 51–53). As a precursor for the biosynthesis of both melanin and catecholamines, tyrosine is central to the tanning and hardening of beetle cuticles (18, 20, 51–53).

Pertaining to the digestive ecology of *C. maculatus*, symbiont acquisition may compensate for the loss of several endogenous cellulases from the insect's genome (42, 43, 54). Relative to other members of the Phytophaga, the bean beetle no longer encodes cellulolytic enzymes belonging to GH families 9, 45, and 48 (41, 42). Alongside pectinases and xylanases, the acquisition of these digestive enzymes is cited as a key innovation that spurred the evolution of herbivory in beetles (41). Our annotation of complementary cellulases belonging to the GH 6 family in the genome of *S. gallinarum* is consistent with the cellulolytic metabolism of the firmicute. By potentially underlying a digestive role for its host, symbiont-produced endoglucanases would complement a range of mannanases and pectinases endogenously retained by *C. maculatus*. Such a division of labor is demonstrated in other Chrysomelidae subfamilies where the loss of insect pectinases is offset following the independent acquisition of foregut-associated pectinolytic symbionts (44–46).

Toward determining the exact mutualistic role of *S. gallinarum*, future efforts will establish a targeted and efficient symbiont-clearing method, coupled with the development of a chemically defined artificial diet. Elucidating the metabolic importance of the symbiont will further our understanding of an economically important insect species and possibly shed light on novel avenues for the control of the bean beetle.

MATERIALS AND METHODS

Rearing conditions and sample collection. A laboratory culture of *C. maculatus* was established using beetles collected in Columbus, OH. The insects were reared in plastic containers (20 by 13 by 12 cm) at room temperature and supplied with cowpea seeds (*V. unguiculata*) *ad libitum*. The grains and rearing cages were autoclaved to minimize exposure to environmental microbes.

To characterize the bacterial community associated with *C. maculatus* during development and to investigate the heritability of the insect's bacterial associates, a cohort of beetles from four different females was established. One replicate per line was collected for every sample type (i.e., larvae, adult females and adult males, and eggs), resulting in a total of four replicates per developmental stage. Eggs were obtained by allowing F_1 females to oviposit on autoclaved glass beads for 24 h. All eggs laid within 48 h by each female were pooled and constituted a single replicate to ensure sufficient DNA extraction yields. For larvae and whole adults, entire individuals were used to extract genomic DNA. To assess whether the gut bacterial symbionts of *C. maculatus* are representative of the community associated with the beetle as a whole, we additionally sampled isolated guts. Prior to dissection, animals were submerged in 0.1% sodium dodecyl sulfate (SDS) and rinsed with sterile water to remove surface contaminants. A continuous gut (foregut, midgut, and hindgut) was dissected under sterile water and placed into individual Eppendorf tubes for DNA extraction.

DNA extraction and 16S rRNA gene sequencing. Insects were euthanized by freezing at -20°C for 15 min. Prior to extraction, egg, larva, and adult samples were surface sterilized with ethanol, subsequently flash-frozen with liquid nitrogen, homogenized with a pestle, and resuspended in 0.5 ml of sterile water. DNA was extracted using a phenol-chloroform protocol according to the instructions at www.beanbeetle.org (accessed January 2021). Subsequently, the extracted DNA was used for sequencing with the Illumina MiSeq platform and paired-end 250-bp technology. Sequencing was performed at Mr. DNA (Shallowater, TX, USA). The V4 variable region of the bacterial 16S rRNA gene was sequenced using the Earth Microbiome Project primer pair 515F and 806R (55). Barcodes were attached to the forward primer. Amplification was performed using the HotStarTaq Plus master mix kit (Qiagen, USA) under the following PCR conditions: 3 min at 94°C , followed by 28 cycles of 30 s at 94°C , 40 s at 53°C , and 1 min at 72°C , with a final 5-min elongation step at 72°C . Amplicons were run in a 2% agarose gel to determine amplification success. Samples were purified using calibrated AMPure XP beads, and purified amplicons were used to construct Illumina DNA libraries.

Bacterial community analysis. The quality of raw sequences was controlled by performing q25 trimming of the ends of reads with Trimmomatic (56). Forward and reverse sequences were joined in Qiime v1 (57) (script `join_paired_ends.py`) and reoriented where necessary. Sequences shorter than 200 bp were removed. Processing of high-quality reads was performed using Qiime v2 2017.4 (58). Joined reads were demultiplexed using the q2-demux plug-in, and forward and reverse primers were removed with q2-cutadapt. Reads were further subjected to a quality-filtering step using DEBLUR (59) to denoise data by setting `-p-trim-length` at 273 bp. Amplicon sequence variants (ASVs) were aligned using mafft (60). In order to build a phylogenetic tree, the alignment was filtered to eliminate highly variable positions that added noise to the tree, which was constructed using fastTree (61) via q2-phylogeny, and rooted at the midpoint. In order to assess the quality of our sequencing depth, our samples were rarefied to 3,000 sequences per sample. After rarefaction, one egg sample was observed to have too few reads and was eliminated from the data set. Taxonomy was assigned to the ASV table using q2-feature-

classifier (62) classify-sklearn against the Greengenes database released in May 2013 (99% sequence similarity) (63). ASVs corresponding to *Archaea*, mitochondria, and chloroplasts were eliminated. In order to facilitate visual representation of the bacterial community, ASVs were grouped according to their taxonomy assignment at 95% sequence similarity (genus level).

Three beta diversity metrics (weighted UniFrac [64], Bray-Curtis dissimilarity, and the Jaccard similarity coefficient), as well as principal coordinates, were calculated using q2-diversity after rarifying samples (subsampling without replacement) to 3,000 sequences per sample. We statistically tested whether ASV association with *C. maculatus* was dependent on life stage, sex, or body site (whole body versus gut) by independently analyzing the matrices with PERMANOVA. Where necessary, the resulting *P* values were adjusted to *q* values for multiple comparisons using Benjamini-Hochberg false discovery rate correction (65). *P* values of <0.05 and *q* values of <0.05 were considered significant.

The ASV table was employed to calculate the “core” microbiome, defined as all the ASVs present in 100% of all samples in each life stage. Taxa shared by all developmental stages were visualized through a Venn diagram generated with the free online tool Venny (66).

Fluorescence *in situ* hybridization. To localize the bacterial symbiotic community within *C. maculatus*, fluorescence *in situ* hybridization (FISH) was performed on semithin section preparations as previously described by Weiss and Kaltenpoth (67). Whole beetles, fixed in 4% paraformaldehyde (PFA) in phosphate-buffered saline (PBS), were embedded in Technovit 8100 (Heraeus Kulzer, Wehrheim, Germany), and semithin sections (8 μ m) were generated on a rotary microtome (Leica RM 2245) using a glass blade. Hybridization was achieved by incubation for 16 h at 50°C with hybridization buffer (0.9 M NaCl, 0.02 M Tris-HCl [pH 8.0], 0.01% SDS) containing 50 μ l/ml of the probe Staph_Callosobruch-Cy5 (GGACTACGGGGTATCTAATCC) targeting the *Callosobruchus*-associated *Staphylococcus* symbiont (500 nM), the general eubacterial probe EUB-3888-Cy3 (GCTGCCTCCCGTAGGAGT) (500 nM), as well as 5 μ g/ml 4',6-diamidino-2-phenylindole (DAPI) for counterstaining of host cell nuclei. Slides were incubated for 20 min in 50°C preheated washing buffer (0.1 M NaCl, 0.02 M Tris-HCl [pH 8.0], 0.01% SDS, 5 mM EDTA), followed by washing with distilled water (dH₂O) for another 20 min. Upon drying at room temperature, Vectashield was applied prior to observation using a Zeiss (Jena, Germany) AxioImager.Z2 fluorescence microscope with Apotome.2.

Culturing gut bacterial isolates and phylogenetic placement. To better understand the possible symbiotic role of *C. maculatus*-associated *S. gallinarum*, the microbe was isolated on culture plates. Insects were euthanized by freezing at -80°C for 5 min. Samples were surface sterilized by submerging single individuals in 10% bleach for 3 s and sterile water for 10 s, followed by submersion in 70% ethanol for 5 s and a final rinse with sterile water for 10 s. Individual beetles were placed in Eppendorf tubes containing 450 μ l of a sterile saline solution (Sigma). Samples were homogenized using a sterile pestle, and debris was pelleted by centrifugation (20 s at 8,000 rpm). One hundred microliters of this mixture was plated on each of the following media and incubated at 30°C: nutrient agar, eosin methylene blue, blood agar, and phenylethyl alcohol agar. Single colonies were further streaked onto LB agar plates to obtain pure cultures that were subsequently stored in glycerol stocks until further use.

Pure isolates were identified via colony PCR using the eubacterial primer pair 27F-1429R (68). The temperature profile was as follows: an initial step of 95°C for 10 min was followed by 36 cycles consisting of 30 s at 95°C, 30 s at 55°C, and an elongation step of 1.5 min at 72°C, followed by 4 min at 72°C. PCR products were visualized in a 1.5% agarose gel. Successful amplicons were sent to Eurofins for sequencing. Taxonomy was assigned to each isolate by comparing each sequence to the NCBI database using BLAST (69).

Symbiont DNA extraction, genome sequencing, and assembly. The genome of a *C. maculatus*-associated *S. gallinarum* isolate from *C. maculatus*' digestive tract was sequenced in order to explore its general features and metabolic capabilities. Genomic DNA was extracted from the isolate using the DNeasy blood and tissue DNA extraction kit (Qiagen), according to the manufacturer's protocol for Gram-positive bacteria. An unsheared DNA library was prepared with an SQK-LSK109 ligation sequencing kit (Oxford Nanopore Technologies). DNA was size selected (enrichment for reads of >3 kb) during the ligation step by washing the sample with long-fragment buffer (Oxford Nanopore Technologies). DNA was sequenced in-house with the Oxford Nanopore MinION sequencer, and base calling was performed with MinKNOW 19.06.8 (Oxford Nanopore Technologies) with the “fast” algorithm. The flow cell used was FLO-FLG001 (Oxford Nanopore Technologies). Genome sequencing resulted in 88,949 reads, an *N*₅₀ of 13,447, and an average read length of 6,857.4, as determined by the “assembly-stats 1.0.1” script, which was run with default parameters (<https://github.com/sanger-pathogens/assembly-stats> [accessed March 2021]). No quality control (QC), error correction, or adapter trimming was performed. A replicate sample was also sequenced with the Illumina HiSeq platform utilizing 150-bp paired-end technology at a depth of ~80 million reads (Omega Bioservices, GA, USA). An Illumina DNA library was prepared using the Kapa HyperPlus kit (Roche) according to the manufacturer's protocol. A hybrid assembly was carried out by combining long Nanopore with short Illumina reads using Unicycler v0.4.8 (70), which automatically circularized the genome and rotated it to DnaA. The genome was confirmed to be complete and visualized by employing Bandage (v0.8.1) with default parameters. Annotation of contigs was performed using PROKKA 1.11 (71). Gene annotations were clustered into Clusters of Orthologous Groups (COG) categories and KO (KEGG Orthology) pathways using eggNOG (72, 73). Carbohydrate-active enzymes were predicted using DIAMOND within the dbCAN2 meta server (74). GC skew values were calculated using the script GC_content.pl by Damien Richard (<https://github.com/DamienFr/> [accessed January 2021]), using default parameters. Genomic data were visualized with Circos (75).

Phylogenetic reconstruction. Phylogenetic inference was performed using a set of 49 universal and highly conserved genes defined by COG and shared by members of the *Firmicutes* phylum (see

Table S3 in the supplemental material). Extracted sequences were aligned using MUSCLE (76), ahead of concatenation. Maximum likelihood (ML) tree inference, under the G+T+I model, was performed using GARLI 2.0 as implemented in the Cipres Science Gateway (77), with 1,000 bootstrap replicates.

Data availability. Genomic sequencing data generated for this article are available in the NCBI and the National Center for Biotechnology Information databases under BioProject accession number PRJNA694570. Amplicon sequencing data and sample metadata are available at https://figshare.com/articles/dataset/16s_rRNA_gene_bacterial_community_profiling_files/14330867. Genome annotation data (gff) are available at https://figshare.com/articles/dataset/gff_file_for_S_gallinarum_s_genome/14340344.

SUPPLEMENTAL MATERIAL

Supplemental material is available online only.

SUPPLEMENTAL FILE 1, XLSX file, 0.1 MB.

ACKNOWLEDGMENTS

This work was supported by the German Science Foundation (BE 6922/1-1 to A.B.), the Smithsonian Institution (to H.S.), the Alexander von Humboldt Foundation (to H.S.), the Max Planck Society (to H.S.), the National Science Foundation (DUE-1821184 to C.W.B.), and the Center for Faculty Development and Excellence Fund for Innovative Teaching at Emory University (to C.W.B.).

The *C. maculatus*-associated *S. gallinarum* strain featured in the genomic analyses was isolated by students in Emory University's introductory biology laboratory as part of the Bean Beetle Microbiome project. We thank Megan Cole, the laboratory course director, for providing the strain.

REFERENCES

- Hagstrum DW, Phillips TW. 2017. Evolution of stored-product entomology: protecting the world food supply. *Annu Rev Entomol* 62:379–397. <https://doi.org/10.1146/annurev-ento-031616-035146>.
- Tuda M, Kagoshima K, Toquenaga Y, Arnqvist G. 2014. Global genetic differentiation in a cosmopolitan pest of stored beans: effects of geography, host-plant usage and anthropogenic factors. *PLoS One* 9:e106268. <https://doi.org/10.1371/journal.pone.0106268>.
- Singh SR, Emden HFV. 1979. Insect pests of grain legumes. *Annu Rev Entomol* 24:255–278. <https://doi.org/10.1146/annurev.en.24.010179.001351>.
- Jackai LEN, Daoust RA. 1986. Insect pests of cowpeas. *Annu Rev Entomol* 31:95–119.
- Southgate BJ. 1979. Biology of the Bruchidae. *Annu Rev Entomol* 24:449–473. <https://doi.org/10.1146/annurev.en.24.010179.002313>.
- Credland PF, Dick KM. 1987. Food consumption by larvae of three strains of *Callosobruchus maculatus* (Coleoptera: Bruchidae). *J Stored Prod Res* 23:31–40. [https://doi.org/10.1016/0022-474X\(87\)90033-6](https://doi.org/10.1016/0022-474X(87)90033-6).
- Hussain MH, Abdel-Aal YAI. 1982. Toxicity of some compounds against the cowpea seed beetle *Callosobruchus maculatus* (Fab.) (Coleoptera: Bruchidae). *Int Pest Control* 24:12–17.
- Deshpande V, Makanur B, Deshpande S, Adiger S, Salimath P. 2011. Quantitative and qualitative losses caused by *Callosobruchus maculatus* in cowpea during seed storage. *Plant Arch* 11:723–731.
- Beck C, Blumer LS. 2021. Advancing undergraduate laboratory education using non-model insect species. *Annu Rev Entomol* 66:485–504. <https://doi.org/10.1146/annurev-ento-062920-095809>.
- Schoof HF. 1941. The effects of various relative humidities on the life processes of the Southern cowpea weevil, *Callosobruchus maculatus* (FABR.) at 30° C., ± 0.8°. *Ecology* 22:297–305. <https://doi.org/10.2307/1929615>.
- Eady PE. 1991. Sperm competition in *Callosobruchus maculatus* (Coleoptera: Bruchidae): a comparison of two methods used to estimate paternity. *Ecol Entomol* 16:45–53. <https://doi.org/10.1111/j.1365-2311.1991.tb00191.x>.
- Patel NH, Condrón BG, Zinn K. 1994. Pair-rule expression patterns of even-skipped are found in both short- and long-germ beetles. *Nature* 367:429–434. <https://doi.org/10.1038/367429a0>.
- Brown EA, Gay L, Vasudev R, Tregenza T, Eady PE, Hosken DJ. 2009. Negative phenotypic and genetic associations between copulation duration and longevity in male seed beetles. *Heredity* (Edinb) 103:340–345. <https://doi.org/10.1038/hdy.2009.80>.
- Kikuchi Y, Hayatsu M, Hosokawa T, Nagayama A, Tago K, Fukatsu T. 2012. Symbiont-mediated insecticide resistance. *Proc Natl Acad Sci U S A* 109:8618–8622. <https://doi.org/10.1073/pnas.1200231109>.
- Itoh H, Tago K, Hayatsu M, Kikuchi Y. 2018. Detoxifying symbiosis: microbe-mediated detoxification of phytotoxins and pesticides in insects. *Nat Prod Rep* 35:434–454. <https://doi.org/10.1039/c7np00051k>.
- Salem H, Bauer E, Strauss AS, Vogel H, Marz M, Kaltenpoth M. 2014. Vitamin supplementation by gut symbionts ensures metabolic homeostasis in an insect host. *Proc Biol Sci* 281:20141838. <https://doi.org/10.1098/rspb.2014.1838>.
- Ceja-Navarro JA, Vega FE, Karaoz U, Hao Z, Jenkins S, Lim HC, Kosina P, Infante F, Northen TR, Brodie EL. 2015. Gut microbiota mediate caffeine detoxification in the primary insect pest of coffee. *Nat Commun* 6:7618. <https://doi.org/10.1038/ncomms8618>.
- Hirota B, Okude G, Anbutso H, Futahashi R, Moriyama M, Meng X-Y, Nikoh N, Koga R, Fukatsu T. 2017. A novel, extremely elongated, and endocellular bacterial symbiont supports cuticle formation of a grain pest beetle. *mBio* 8:e01482-17. <https://doi.org/10.1128/mBio.01482-17>.
- Vigneron A, Masson F, Vallier A, Balmand S, Rey M, Vincent-Monégat C, Aksoy E, Aubailly-Giraud E, Zaidman-Rémy A, Heddi A. 2014. Insects recycle endosymbionts when the benefit is over. *Curr Biol* 24:2267–2273. <https://doi.org/10.1016/j.cub.2014.07.065>.
- Engl T, Eberl N, Gorse C, Krüger T, Schmidt THP, Plarre R, Adler C, Kaltenpoth M. 2018. Ancient symbiosis confers desiccation resistance to stored grain pest beetles. *Mol Ecol* 27:2095–2108. <https://doi.org/10.1111/mec.14418>.
- Sevim A, Sevim E, Demirci M, Sandalli C. 2016. The internal bacterial diversity of stored product pests. *Ann Microbiol* 66:749–764. <https://doi.org/10.1007/s13213-015-1155-5>.
- Akami M, Njintang NY, Gbaye OA, Andongma AA, Rashid MA, Niu C-Y, Nukenine EN. 2019. Gut bacteria of the cowpea beetle mediate its resistance to dichlorvos and susceptibility to *Lippia adoensis* essential oil. *Sci Rep* 9:6435. <https://doi.org/10.1038/s41598-019-42843-1>.
- Sreerag RS, Jayaprakas CA, Ragesh L, Kumar SN. 2014. Endosymbiotic bacteria associated with the mealy bug, *Rhizoecus amorphophalli* (Hemiptera: Pseudococcidae). *Int Sch Res Notices* 2014:268491. <https://doi.org/10.1155/2014/268491>.
- Prakash R. 2011. Isolation of bacteria from *Callosobruchus maculatus*, coleopteran pest of stored products. *J Ecotoxicol Environ Monit* 21:541–544.

25. Sudakaran S, Salem H, Kost C, Kaltenpoth M. 2012. Geographical and ecological stability of the symbiotic mid-gut microbiota in European firebugs, *Pyrrhocoris apterus* (Hemiptera, Pyrrhocoridae). *Mol Ecol* 21:6134–6151. <https://doi.org/10.1111/mec.12027>.
26. Engel P, Moran NA. 2013. The gut microbiota of insects—diversity in structure and function. *FEMS Microbiol Rev* 37:699–735. <https://doi.org/10.1111/1574-6976.12025>.
27. Köhler T, Dietrich C, Scheffrahn RH, Brune A. 2012. High-resolution analysis of gut environment and bacterial microbiota reveals functional compartmentation of the gut in wood-feeding higher termites (*Nasutitermes* spp.). *Appl Environ Microbiol* 78:4691–4701. <https://doi.org/10.1128/AEM.00683-12>.
28. Ryu J-H, Kim S-H, Lee H-Y, Bai JY, Nam Y-D, Bae J-W, Lee DG, Shin SC, Ha E-M, Lee W-J. 2008. Innate immune homeostasis by the homeobox gene caudal and commensal-gut mutualism in *Drosophila*. *Science* 319:777–782. <https://doi.org/10.1126/science.1149357>.
29. Bauer E, Salem H, Marz M, Vogel H, Kaltenpoth M. 2014. Transcriptomic immune response of the cotton stainer *Dysdercus fasciatus* to experimental elimination of vitamin-supplementing intestinal symbionts. *PLoS One* 9:e114865. <https://doi.org/10.1371/journal.pone.0114865>.
30. Ha E-M, Oh C-T, Ryu J-H, Bae Y-S, Kang S-W, Jang I, Brey PT, Lee W-J. 2005. An antioxidant system required for host protection against gut infection in *Drosophila*. *Dev Cell* 8:125–132. <https://doi.org/10.1016/j.devcel.2004.11.007>.
31. Argemi X, Matelska D, Ginalski K, Riegel P, Hansmann Y, Bloom J, Pestel-Caron M, Dahyot S, Lebeurre J, Prévost G. 2018. Comparative genomic analysis of *Staphylococcus lugdunensis* shows a closed pan-genome and multiple barriers to horizontal gene transfer. *BMC Genomics* 19:621. <https://doi.org/10.1186/s12864-018-4978-1>.
32. Rocha EPC, Danchin A. 2003. Gene essentiality determines chromosome organisation in bacteria. *Nucleic Acids Res* 31:6570–6577. <https://doi.org/10.1093/nar/gkg859>.
33. Takeuchi F, Watanabe S, Baba T, Yuzawa H, Ito T, Morimoto Y, Kuroda M, Cui L, Takahashi M, Ankaï A, Baba S, Fukui S, Lee JC, Hiramatsu K. 2005. Whole-genome sequencing of *Staphylococcus haemolyticus* uncovers the extreme plasticity of its genome and the evolution of human-colonizing staphylococcal species. *J Bacteriol* 187:7292–7308. <https://doi.org/10.1128/JB.187.21.7292-7308.2005>.
34. Shibuya R, Uehara Y, Baba T, Teruya K, Satou K, Hirano T, Kirikae T, Hiramatsu K. 2020. Complete genome sequence of a methicillin-resistant *Staphylococcus lugdunensis* strain and characteristics of its staphylococcal cassette chromosome *mec*. *Sci Rep* 10:8682. <https://doi.org/10.1038/s41598-020-65632-7>.
35. Devriese LA, Poutrel B, Kilpper-Balz R, Schleifer KH. 1983. *Staphylococcus gallinarum* and *Staphylococcus caprae*, two new species from animals. *Int J Syst Bacteriol* 33:480–486. <https://doi.org/10.1099/00207713-33-3-480>.
36. Becker K, Heilmann C, Peters G. 2014. Coagulase-negative staphylococci. *Clin Microbiol Rev* 27:870–926. <https://doi.org/10.1128/CMR.00109-13>.
37. Adegoké GO. 1986. Comparative characteristics of *Staphylococcus sciuri*, *Staphylococcus lentus* and *Staphylococcus gallinarum* isolated from healthy and sick hosts. *Vet Microbiol* 11:185–189. [https://doi.org/10.1016/0378-1135\(86\)90019-2](https://doi.org/10.1016/0378-1135(86)90019-2).
38. Saranya M, Krishnamoorthy S, Muruges K. 2019. Fortification of mulberry leaves with indigenous probiotic bacteria on larval growth and economic traits of silkworm (*Bombyx mori* L.). *J Entomol Zool Stud* 7:780–784.
39. Ateyyat MA, Shatnawi M, Al-Mazra'awi M. 2010. Isolation and identification of culturable forms of bacteria from the sweet potato whitefly *Bemisia [sic] tabaci* Genn. (Homoptera: Aleyrodidae) in Jordan. *Turk J Agric For* 34:225–234.
40. Kirsch R, Gramzow L, Theißen G, Siegfried BD, Ffrench-Constant RH, Heckel DG, Pauchet Y. 2014. Horizontal gene transfer and functional diversification of plant cell wall degrading polygalacturonases: key events in the evolution of herbivory in beetles. *Insect Biochem Mol Biol* 52:33–50. <https://doi.org/10.1016/j.ibmb.2014.06.008>.
41. McKenna DD, Shin S, Ahrens D, Balke M, Beza-Beza C, Clarke DJ, Donath A, Escalona HE, Friedrich F, Letsch H, Liu S, Maddison D, Mayer C, Misof B, Murin PJ, Niehuis O, Peters RS, Podsiadlowski L, Pohl H, Scully ED, Yan EV, Zhou X, Šliipiński A, Beutel RG. 2019. The evolution and genomic basis of beetle diversity. *Proc Natl Acad Sci U S A* 116:24729–24737. <https://doi.org/10.1073/pnas.1909655116>.
42. Pauchet Y, Wilkinson P, Chauhan R, Ffrench-Constant RH. 2010. Diversity of beetle genes encoding novel plant cell wall degrading enzymes. *PLoS One* 5:e15635. <https://doi.org/10.1371/journal.pone.0015635>.
43. Busch A, Kunert G, Heckel DG, Pauchet Y. 2017. Evolution and functional characterization of CAZymes belonging to subfamily 10 of glycoside hydrolase family 5 (GH5_10) in two species of phytophagous beetles. *PLoS One* 12:e0184305. <https://doi.org/10.1371/journal.pone.0184305>.
44. Salem H, Bauer E, Kirsch R, Berasategui A, Cripps M, Weiss B, Koga R, Fukumori K, Vogel H, Fukatsu T, Kaltenpoth M. 2017. Drastic genome reduction in an herbivore's pectinolytic symbiont. *Cell* 171:1520–1531. e13. <https://doi.org/10.1016/j.cell.2017.10.029>.
45. Salem H, Kirsch R, Pauchet Y, Berasategui A, Fukumori K, Moriyama M, Cripps M, Windsor D, Fukatsu T, Gerardo NM. 2020. Symbiotic digestive range reflects host plant breadth in herbivorous beetles. *Curr Biol* 30:2875–2886.e4. <https://doi.org/10.1016/j.cub.2020.05.043>.
46. Reis F, Kirsch R, Pauchet Y, Bauer E, Bilz LC, Fukumori K, Fukatsu T, Kölsch G, Kaltenpoth M. 2020. Bacterial symbionts support larval sap feeding and adult folivory in (semi-)aquatic reed beetles. *Nat Commun* 11:2964. <https://doi.org/10.1038/s41467-020-16687-7>.
47. Fraenkel G, Blewett M. 1943. Intracellular symbionts of insects as a source of vitamins. *Nature* 152:506–507. <https://doi.org/10.1038/152506a0>.
48. Blewett M, Fraenkel G. 1944. Intracellular symbiosis and vitamin requirements of two insects, *Lasioderma serricorne* and *Sitodrepa panicea*. *Proc R Soc Lond B* 132:212–221.
49. Wicker C. 1983. Differential vitamin and choline requirements of symbiotic and aposymbiotic *S. oryzae* (Coleoptera: Curculionidae). *Comp Biochem Physiol A Physiol* 76:177–182. [https://doi.org/10.1016/0300-9629\(83\)90311-0](https://doi.org/10.1016/0300-9629(83)90311-0).
50. Noh MY, Muthukrishnan S, Kramer KJ, Arakane Y. 2016. Cuticle formation and pigmentation in beetles. *Curr Opin Insect Sci* 17:1–9. <https://doi.org/10.1016/j.cois.2016.05.004>.
51. Anbutso H, Moriyama M, Nikoh N, Hosokawa T, Futahashi R, Tanahashi M, Meng X-Y, Kuriwada T, Mori N, Oshima K, Hattori M, Fujie M, Satoh N, Maeda T, Shigenobu S, Koga R, Fukatsu T. 2017. Small genome symbiont underlies cuticle hardness in beetles. *Proc Natl Acad Sci U S A* 114: E8382–E8391. <https://doi.org/10.1073/pnas.1712857114>.
52. Kuriwada T, Hosokawa T, Kumano N, Shiromoto K, Haraguchi D, Fukatsu T. 2010. Biological role of *Nardonella* endosymbiont in its weevil host. *PLoS One* 5:e13101. <https://doi.org/10.1371/journal.pone.0013101>.
53. Salem H, Kaltenpoth M. Beetle-bacterial symbioses: endless forms most functional. *Annu Rev Entomol*, in press.
54. Sayadi A, Martínez Barrio A, Immonen E, Dainat J, Berger D, Tellgren-Roth C, Nystedt B, Arnqvist G. 2019. The genomic footprint of sexual conflict. *Nat Ecol Evol* 3:1725–1730. <https://doi.org/10.1038/s41559-019-1041-9>.
55. Caporaso JG, Lauber CL, Walters WA, Berg-Lyons D, Huntley J, Fierer N, Owens SM, Betley J, Fraser L, Bauer M, Gormley N, Gilbert JA, Smith G, Knight R. 2012. Ultra-high-throughput microbial community analysis on the Illumina HiSeq and MiSeq platforms. *ISME J* 6:1621–1624. <https://doi.org/10.1038/ismej.2012.8>.
56. Bolger AM, Lohse M, Usadel B. 2014. Trimmomatic: a flexible trimmer for Illumina sequence data. *Bioinformatics* 30:2114–2120. <https://doi.org/10.1093/bioinformatics/btu170>.
57. Caporaso JG, Kuczynski J, Stombaugh J, Bittinger K, Bushman FD, Costello EK, Fierer N, Peña AG, Goodrich JK, Gordon JI, Huttley GA, Kelley ST, Knights D, Koenig JE, Ley RE, Lozupone CA, McDonald D, Mueggler BD, Pirrung M, Reeder J, Sevinsky JR, Turnbaugh PJ, Walters WA, Widmann J, Yatsunenko T, Zaneveld J, Knight R. 2010. QIIME allows analysis of high-throughput community sequencing data. *Nat Methods* 7:335–336. <https://doi.org/10.1038/nmeth.f.303>.
58. Bolyen E, Rideout JR, Dillon MR, Bokulich NA, Abnet CC, Al-Ghalith GA, Alexander H, Alm EJ, Arumugam M, Asnicar F, Bai Y, Bisanz JE, Bittinger K, Brejnrod A, Brislawn CJ, Brown CT, Callahan BJ, Caraballo-Rodríguez AM, Chase J, Cope EK, Da Silva R, Diener C, Dorrestein PC, Douglas GM, Durall DM, Duvallet C, Edwards CF, Ernst M, Estaki M, Fouquier J, Gauglitz JM, Gibbons SM, Gibson DL, Gonzalez A, Gorlick K, Guo J, Hillmann B, Holmes S, Holste H, Huttenhower C, Huttley GA, Janssen S, Jarmusch AK, Jiang L, Kaehler BD, Kang KB, Keefe CR, Keim P, Kelley ST, Knights D, et al. 2019. Reproducible, interactive, scalable and extensible microbiome data science using QIIME 2. *Nat Biotechnol* 37:852–857. <https://doi.org/10.1038/s41587-019-0209-9>.
59. Amir A, McDonald D, Navas-Molina JA, Kopylova E, Morton JT, Xu ZZ, Kightley EP, Thompson LR, Hyde ER, Gonzalez A, Knight R. 2017. Deblur rapidly resolves single-nucleotide community sequence patterns. *mSystems* 2:e00191-16. <https://doi.org/10.1128/mSystems.00191-16>.
60. Katoh K, Misawa K, Kuma K, Miyata T. 2002. MAFFT: a novel method for rapid multiple sequence alignment based on fast Fourier transform. *Nucleic Acids Res* 30:3059–3066. <https://doi.org/10.1093/nar/gkf436>.

61. Price MN, Dehal PS, Arkin AP. 2010. FastTree 2—approximately maximum-likelihood trees for large alignments. *PLoS One* 5:e9490. <https://doi.org/10.1371/journal.pone.0009490>.
62. Bokulich NA, Kaehler BD, Rideout JR, Dillon M, Bolyen E, Knight R, Huttley GA, Gregory Caporaso J. 2018. Optimizing taxonomic classification of marker-gene amplicon sequences with QIIME 2's q2-feature-classifier plugin. *Microbiome* 6:90. <https://doi.org/10.1186/s40168-018-0470-z>.
63. McDonald D, Price MN, Goodrich J, Nawrocki EP, DeSantis TZ, Probst A, Andersen GL, Knight R, Hugenholtz P. 2012. An improved Greengenes taxonomy with explicit ranks for ecological and evolutionary analyses of bacteria and archaea. *ISME J* 6:610–618. <https://doi.org/10.1038/ismej.2011.139>.
64. Lozupone C, Lladser ME, Knights D, Stombaugh J, Knight R. 2011. UniFrac: an effective distance metric for microbial community comparison. *ISME J* 5:169–172. <https://doi.org/10.1038/ismej.2010.133>.
65. Benjamini Y, Hochberg Y. 1995. Controlling the false discovery rate: a practical and powerful approach to multiple testing. *J R Stat Soc Series B Stat Methodol* 57:289–300. <https://doi.org/10.1111/j.2517-6161.1995.tb02031.x>.
66. Oliveros J. 2007. VENNY. An interactive tool for comparing lists with Venn diagrams.
67. Weiss B, Kaltenpoth M. 2016. Bacteriome-localized intracellular symbionts in pollen-feeding beetles of the genus *Dasytes* (Coleoptera, Dasytidae). *Front Microbiol* 7:1486. <https://doi.org/10.3389/fmicb.2016.01486>.
68. Frank JA, Reich CI, Sharma S, Weisbaum JS, Wilson BA, Olsen GJ. 2008. Critical evaluation of two primers commonly used for amplification of bacterial 16S rRNA genes. *Appl Environ Microbiol* 74:2461–2470. <https://doi.org/10.1128/AEM.02272-07>.
69. Altschul SF, Gish W, Miller W, Myers EW, Lipman DJ. 1990. Basic local alignment search tool. *J Mol Biol* 215:403–410. [https://doi.org/10.1016/S0022-2836\(05\)80360-2](https://doi.org/10.1016/S0022-2836(05)80360-2).
70. Wick RR, Judd LM, Gorrie CL, Holt KE. 2017. Unicycler: resolving bacterial genome assemblies from short and long sequencing reads. *PLoS Comput Biol* 13:e1005595. <https://doi.org/10.1371/journal.pcbi.1005595>.
71. Seemann T. 2014. Prokka: rapid prokaryotic genome annotation. *Bioinformatics* 30:2068–2069. <https://doi.org/10.1093/bioinformatics/btu153>.
72. Huerta-Cepas J, Forslund K, Coelho LP, Szklarczyk D, Jensen LJ, von Mering C, Bork P. 2017. Fast genome-wide functional annotation through orthology assignment by eggNOG-Mapper. *Mol Biol Evol* 34:2115–2122. <https://doi.org/10.1093/molbev/msx148>.
73. Huerta-Cepas J, Szklarczyk D, Heller D, Hernández-Plaza A, Forslund SK, Cook H, Mende DR, Letunic I, Rattei T, Jensen LJ, von Mering C, Bork P. 2019. eggNOG 5.0: a hierarchical, functionally and phylogenetically annotated orthology resource based on 5090 organisms and 2502 viruses. *Nucleic Acids Res* 47:D309–D314. <https://doi.org/10.1093/nar/gky1085>.
74. Zhang H, Yohe T, Huang L, Entwistle S, Wu P, Yang Z, Busk PK, Xu Y, Yin Y. 2018. dbCAN2: a meta server for automated carbohydrate-active enzyme annotation. *Nucleic Acids Res* 46:W95–W101. <https://doi.org/10.1093/nar/gky418>.
75. Krzywinski MI, Schein JE, Birol I, Connors J, Gascoyne R, Horsman D, Jones SJ, Marra MA. 2009. Circos: an information aesthetic for comparative genomics. *Genome Res* 19:1639–1645. <https://doi.org/10.1101/gr.092759.109>.
76. Edgar RC. 2004. MUSCLE: multiple sequence alignment with high accuracy and high throughput. *Nucleic Acids Res* 32:1792–1797. <https://doi.org/10.1093/nar/gkh340>.
77. Bazinet AL, Zwickl DJ, Cummings MP. 2014. A gateway for phylogenetic analysis powered by grid computing featuring GARLI 2.0. *Syst Biol* 63:812–818. <https://doi.org/10.1093/sysbio/syu031>.
78. Berasategui A, Salem H. 2020. Microbial determinants of folivory in insects, chapter 13. *In* Bosch TCG, Hadfield MG (ed), *Cellular dialogues in the holobiont*. CRC Press, Boca Raton, FL.